Characterisation of Balcony Spill Plume Entrainment using Physical Scale Modelling

ROGER HARRISON and MICHAEL SPEARPOINT
Department of Civil and Natural Resources Engineering
University of Canterbury
Christchurch, New Zealand

ABSTRACT

Smoke management design for buildings such as atria and multi-level complexes often requires consideration of smoke produced from a balcony spill plume. This work provides new experimental data to characterise entrainment of air into a balcony spill plume using the approach of physical scale modelling. For a balcony spill plume without entrainment of air into the ends, this work has demonstrated that existing simplified design formulae generally apply for plumes generated from a range of fire compartment geometries. A further simplified design formula is proposed for this type of plume. For a balcony spill plume with entrainment of air into the free ends, the rate of entrainment appears to be specifically dependent on the characteristics of the layer flow below the balcony edge. A simplified design formula is proposed by developing a general empirical expression to describe entrainment of air into the ends of the plume. This work goes some way to explain and reconcile differences in entrainment reported between previous studies and provides improved guidance to designers of smoke management systems.

KEYWORDS: smoke management, balcony spill plume, entrainment

NOMENCLATURE LISTING

Term

C	Coefficient in Equation 2 (kg $m^{1/3}s^{-1}kW^{-1/3}$)
d	Depth of gas layer (m)
$\dot{m}$	Mass flow rate of gases (kgs^{-1})
$\dot{Q}_c$	Convective heat flow of gases (kW)
$\dot{Q}_t$	Total heat output of the fire (kW)
W	Lateral extent of layer at the balcony edge (m)
z	Height of rise of plume above balcony (m)
z_0	Height of virtual source below balcony (m)

Greek

α	Regression coefficient
β	Regression coefficient
γ	Regression coefficient

subscripts

b	Property of layer below balcony edge
ends	Property of the ends of the plume
p	Property of the spill plume
2D	Property of the 2-D plume
3D	Property of the 3-D plume

INTRODUCTION

The design of smoke management systems for buildings such as atria, covered shopping malls and sports arenas require appropriate calculation methods to predict the volume of smoky gases produced in the event of a fire. In design, consideration is often given to entrainment of air into a smoke flow from a compartment opening that subsequently spills at a balcony edge and then rises into an adjacent atrium void. This type of thermal plume is commonly known as a balcony spill plume. There are several calculation methods available for the balcony spill plume, which range from semi-empirical simplified design formulae [1-5] to more complex theories [6,7]. There has been much controversy over the validity of various calculation methods for the balcony spill plume and there are considerable differences in the calculated smoke production rates predicted using these methods [1]. This paper aims to provide information regarding balcony spill plume entrainment using the approach of physical scale modelling. New experimental data has been obtained to rigorously characterise balcony spill plume entrainment by varying the type of plume, fire compartment geometry, fire size and height of rise of plume. Entrainment has been characterised for balcony spill plumes with and without entrainment of air into the ends. In general, this paper seeks to provide a better understanding of spill plume entrainment in an attempt to resolve and reconcile the differences from previous studies and to provide improved guidance to designers of smoke management systems.

FIRE SAFETY SCIENCE–PROCEEDINGS OF THE NINTH INTERNATIONAL SYMPOSIUM, pp. 727-738
 / DOI:10.3801/IAFSS.FSS.9-727

PHYSICAL SCALE MODELLING

The approach of physical scale modelling is well established and has been used in many studies of smoke movement in buildings. The approach described in this paper follows that primarily developed at the Fire Research Station in the UK [8,9] and takes the form of reduced scale fires within a physical model. This approach is also described by Klote and Milke [10]. Measurements are generally made of temperature, velocity and gas concentrations, in addition to visual observations. Measurements can be extrapolated to full scale using the appropriate scaling laws. To ensure that the results can be extrapolated to full scale, the physical scale model used in this study was designed to meet the scaling principles set out by Thomas et al [8]. This is effectively a modified Froude number scaling and requires that the equivalent flows are fully turbulent on both full and model scale.

THE EXPERIMENT

The apparatus used for this work was a $1/10^{th}$ physical scale model (see Figure 1). The model simulated a fire within a room adjacent to an atrium void, and consisted of two main units, the fire compartment and a smoke collecting hood. The model employed a similar technique to that used by Zukoski et al [11] to measure entrainment of air into unbounded axisymmetric plumes. The fire compartment was constructed from 25 mm thick Ceramic Fibre Insulation (CFI) board with a 1 mm thick steel substrate on each external face. The dimensions of the fire compartment were 1.0 by 1.0 by 0.5 m high. The height of the compartment opening was equal to the height of the compartment. The width of the compartment opening was varied by inserting walls of equal width at either end of the opening. The inserted walls had widths of 0.1, 0.2, 0.3 and 0.4 m and were constructed from 25 mm thick CFI board with a 1 mm thick steel substrate on the non-fire side of the compartment. A 2.0 m long and 0.3 m broad balcony constructed from 10 mm thick CFI board with a 1 mm thick steel substrate on its upper face was attached to the fire compartment opening. The balcony extended 0.5 m beyond each side of the fire compartment. For those tests examining balcony spill plumes without entrainment of air into the ends (i.e. the 2-D plume), screens were suspended from the ceiling of the collecting hood, in line with each side of the fire compartment opening, to prevent lateral spread of the plume both below and above the balcony. These screens prevented air from entering the ends of the plume over its full height of rise. The dimensions of these screens were 1.2 m wide by 1.4 m high, made from 10 mm thick CFI board with a 1 mm thick steel sheet substrate on the external face. The screens projected across the breadth of the balcony and continued 0.9 m beyond the balcony edge. The screens projected 0.3 m below the balcony and 1.1 m above the balcony. Those tests which examined balcony spill plumes with entrainment of air into the ends of the plume (i.e. the 3-D plume), used channelling screens which were only located beneath the balcony to prevent lateral spread under the balcony. The screens were located in line with each side of the fire compartment opening and projected across the full breadth of the balcony. The screens were made from 10 mm thick CFI board with a 1 mm thick steel substrate on the external face. The screens used were either 0.2 or 0.3 m deep, depending on the compartment geometry and fire size examined. The side walls of the smoke collecting hood were generally constructed from 10 mm thick CFI board with a 1 mm thick steel sheet substrate on each external face. However, one of the side walls was constructed from 10 mm thick transparent acrylic sheet to enable visual observations to be made of the smoke layer within the collecting hood. The model was designed such that the walls could freely move in a vertical direction within a supporting steel frame. This enabled each wall to be moved independently to just below the base of the observed smoke layer in the hood (approximately 60 mm below) allowing unrestricted fresh air to be entrained into the rising plume. This effectively simulated an unbounded balcony spill plume and prevented warming of the air beneath the observed smoke layer. The supporting steel frame was designed such that each side wall could contain up to two, smaller, modular walls each 2.0 m wide by 1.2 m high, which could be bolted together. This would then form a single wall on each face when examining deep smoke layers within the collecting hood. The mechanical smoke exhaust system from the hood consisted of a 0.44 m diameter bifurcated fan attached to the hood exhaust vent using temperature resistant flexible ducting. The gases were exhausted to the outside of the laboratory through flexible ducting connected to the exhaust end of the fan. The fan speed was controllable, which enabled different exhaust rates, and hence, variation in the height of rise of the plume to be examined. The fire source was generated by supplying Industrial Methylated Spirits into a metal tray within the fire compartment at a controlled and measured rate. The tray was 0.25 by 0.25 by 0.015 m high.

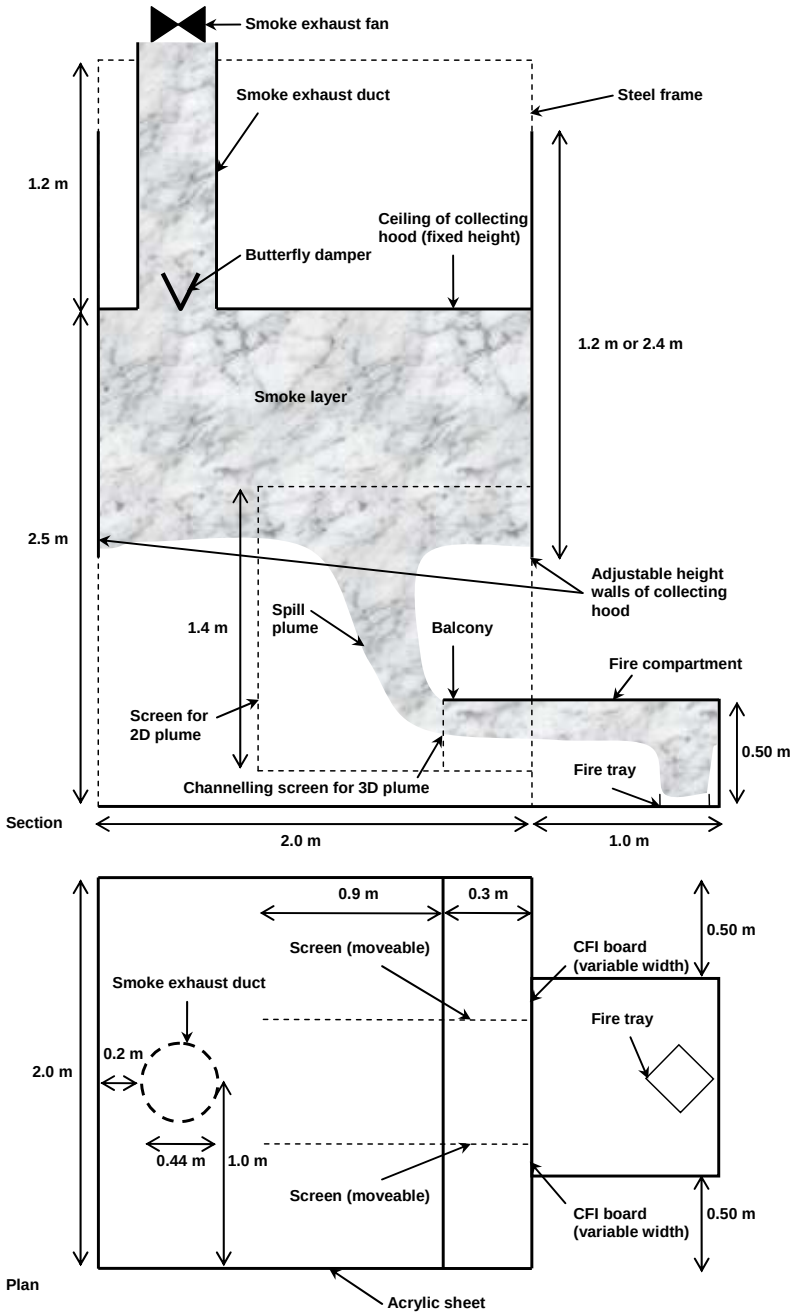

Fig. 1. Schematic Drawing of the 1/10th Physical Scale Model.

The hot gases produced from the fire were visualised by injecting smoke from a commercial smoke generator into the fire compartment. This highlighted the flowing gas layer from the compartment and the subsequent spill plume and smoke layer in the collecting hood. The gas temperatures in the model were measured using 0.5 mm diameter bare wire chromel/alumel (K-type) thermocouples. Thermocouples were positioned at various locations in the model as follows: two columns of 15 thermocouples located within the smoke exhaust hood; one column of 18 thermocouples located centrally beneath the balcony edge; an array of 21 thermocouple across the entire balcony edge, projecting 10 mm below the edge; an array of five thermocouples in the throat of the exhaust vent; one thermocouple located centrally within the smoke exhaust duct, 5.0 m downstream of the exhaust vent; two thermocouples, one located next to each of two pitot-static tubes, when measuring velocity profiles of the smoke layer below the balcony edge. A

perforated gas sampling tube was located in the exhaust duct, 5.0 m downstream of the vent in the smoke exhaust hood. This enabled measurement of the CO_2 gas concentration in the duct to be made using an infra red gas analyser. The mass flow rate of gases entering the buoyant gas layer in the smoke collecting hood and therefore leaving the hood, was found by using a CO_2 tracer gas technique and calculation method described by Marshall [9]. Vertical velocity and temperature profiles of the buoyant gas layer flow below the balcony edge were made using two pitot-static tubes and a thermocouple. The pitot-static tubes were each located a distance of one-third of the compartment opening width from each side of the opening. Each pitot-tube was connected to a sensitive differential pressure transducer. Gas velocity measurements were made every 10 mm below the balcony edge until the base of the smoke layer was reached (i.e. from visual observations and until a negative flow, from the inflow, was measured). This measurement, in addition to the temperature profiles, enabled the mass flow rate and convective heat flow of the gas layer below the balcony edge to be determined. A series of 97 experiments was carried out as part of an extensive parametric analysis to characterise entrainment of air into a balcony spill plume. For the vast majority of the experiments, a balcony spill plume with air entrainment into the free ends was examined. For these experiments examining the 3-D spill plume, the total heat output of the fire was varied, three fire sizes were examined of 5, 10 and 15 kW respectively. This equates to a fire size of 1.6, 3.2 and 4.7 MW respectively for a full scale equivalent using the scaling laws. Varying the total heat output of the fire in turn varied the mass flow rate, convective heat flow and depth of the gas layer below the balcony edge. The height of rise of plume above the balcony was also varied, with six different heights examined between 0 to 1.25 m. The width of the fire compartment opening was varied, with widths of 0.2, 0.4, 0.6, 0.8 and 1.0 m examined. Selected experiments were carried out for a balcony spill plume without air entrainment into the free ends to confirm and extend findings from previous work. For these experiments, the height of rise of plume above the balcony edge was varied, with five different heights examined between 0 to 1.02 m. The width of the fire compartment opening was varied, with widths of 0.2, 0.4, 0.6, 0.8 and 1.0 m examined. The total heat output of the fire remained fixed at 10 kW for the experiments without end entrainment.

ANALYSIS

The analysis of 2-D spill plumes often utilises the weak line plume theory described by Lee and Emmons [12]. The plume is assumed to rise from a virtual line source located at a distance below the balcony edge, and makes the assumption of self-similar profiles across the plume (e.g. Gaussian profiles) in terms of velocity and temperature. A constant entrainment coefficient is assumed, providing linearity between the mass flow rate of gases and the height of rise of the plume. Thomas et al [4] and Poreh et al [5] have determined simplified spill plume design formulae for the 2-D plume. Thomas et al used a rigorous dimensional analysis to develop a simplified spill plume model in the form given by Equation 1. This method does not make the assumption of self-similar flow profiles or a constant entrainment coefficient.

$$\frac{\dot{m}'_p}{\dot{Q}'_c} = \alpha \frac{z}{\dot{Q}'^{2/3}_c} + \beta \frac{\dot{m}'_b}{\dot{Q}'_c} + \gamma \qquad \text{where, } \dot{m}'_p = \frac{\dot{m}_p}{W}, \quad \dot{m}'_b = \frac{\dot{m}_b}{W}, \quad \dot{Q}'_c = \frac{\dot{Q}_c}{W} \tag{1}$$

Poreh et al followed a similar approach to Lee and Emmons, and deduced the following simplified design formula given by Equation 2.

$$\frac{\dot{m}'_p - \dot{m}'_b}{\dot{Q}'_c} = C\left(\frac{z + z_0}{\dot{Q}'^{2/3}_c}\right) \tag{2}$$

When expressed in this form, the Poreh et al method deals with entrainment into the turning region of the plume, as the layer flow rotates at the balcony edge, by assuming it is the same as the entrainment into the virtual region of the plume, with the virtual origin assumed to be located at the base of the gas layer below the balcony edge (i.e. $z_0 = d_b$). These methods will be used to analyse the experimental data from this study for the 2-D plume and the 3-D plume by encompassing the additional entrainment into the ends of the plume into the empirical entrainment coefficient(s).

RESULTS AND DISCUSSION

Balcony Spill Plume without Entrainment of Air into the Ends – The 2-D Plume

Previous 1/10th physical scale modelling work, from separate studies described by Marshall and Harrison [13] has provided data to characterise entrainment of air into a 2-D spill plume. From these data Thomas et al [4] determined, according to Equation 1, that;

$$\frac{\dot{m}'_{p,2D}}{\dot{Q}'_c} = 0.16\frac{z}{\dot{Q}'^{2/3}_c} + 1.2\frac{\dot{m}'_b}{\dot{Q}'_c} + 0.0027 \tag{3}$$

Poreh et al [5] determined from the same data, according to Equation 2, that;

$$\frac{\dot{m}'_{p,2D} - \dot{m}'_b}{\dot{Q}'_c} = 0.16\left(\frac{z + d_b}{\dot{Q}'^{2/3}_c}\right) \tag{4}$$

Equations 3 and 4 were determined for fires with $\dot{Q}_c$ ranging between 6 to 34 kW. However, W was fixed in these experiments at 0.91 m. Therefore, for this study, a selected number of experiments were carried out to determine if Equations 3 and 4 also apply for a range of W. Figure 2 shows the data obtained from this study and previous data by Marshall and Harrison [13], plotted in a form consistent with the dimensional analysis given by Thomas et al [4]. A line representing Equation 3 is also shown for a mid range value of $\dot{Q}_c$ from the Marshall and Harrison data, as it is weakly dependent on $\dot{Q}_c$.

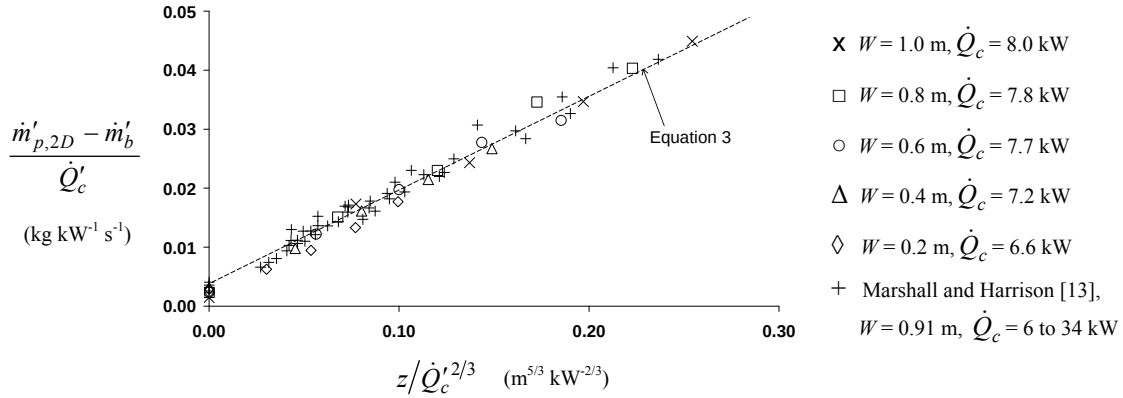

Fig. 2. Comparison of mass flow rate with respect to height of rise according to Thomas et al [4]

Figure 2 shows that all the data follow a common linear relationship, which appears to be independent of $\dot{Q}_c$ and W. The intercept on the vertical axis represents the amount of entrainment in the turning region of the plume. The same data are plotted in Figure 3, according to the method by Poreh et al [5], including a line representing Equation 4. Figures 2 and 3 indicate that the data from this study, obtained from a range of W, is broadly consistent with the data from previous work. Performing linear regression for each complete data set shown in Figures 2 and 3 gives $\alpha = 0.163$ and $C = 0.159$ with standard errors of 0.003 and 0.001 respectively. Therefore, the additional data from this study is consistent with the dominant regression coefficients in Equations 3 and 4 being equal (within 1 standard error), with a value of 0.16. It appears that Equations 3 and 4 can generally be applied for 2-D spill plumes. The difference between them is the term(s) describing the entrainment of air into the flow below the balcony edge (i.e. the mass flow rate in the plume at $z = 0$). Existing experimental data describing entrainment into the plume at $z = 0$ is particularly sparse and has not been characterised in a robust manner. Therefore, in this work, a more extensive data set from 20 experiments was obtained for entrainment at $z = 0$ in an attempt to characterise and decouple entrainment into the flow below the balcony edge. Figure 4 shows a plot of $\dot{m}'_p/\dot{Q}'_c$ versus $\dot{m}'_b/\dot{Q}'_c$ at $z = 0$, consistent with the dimensional analysis by Thomas et al [4].

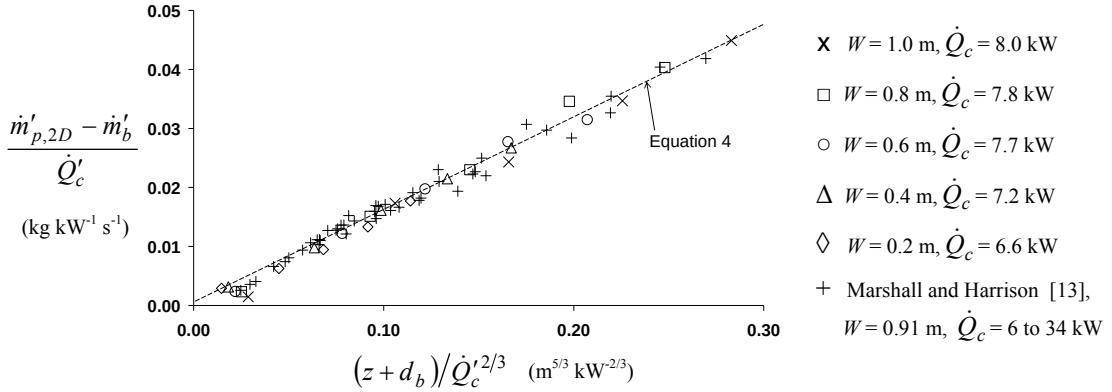

Fig. 3. Comparison of mass flow rate with respect to height of rise according to Poreh et al [5]

The data shown in Figure 4 was from those tests which had channelling screens used for the 2-D plume (screens both above and below the balcony) and those screens used for the 3-D plume (screens only below the balcony), as at z = 0 it is expected that the effect of end entrainment into the rotation region will be negligible for the 3-D plume scenario (also assumed by Thomas et al [4]). Data from previous work by Harrison and Spearpoint [1] and Marshall and Harrison [13], obtained at z = 0, is also included in the analysis. The data is presented in terms of the time averaged mean value with associated standard errors.

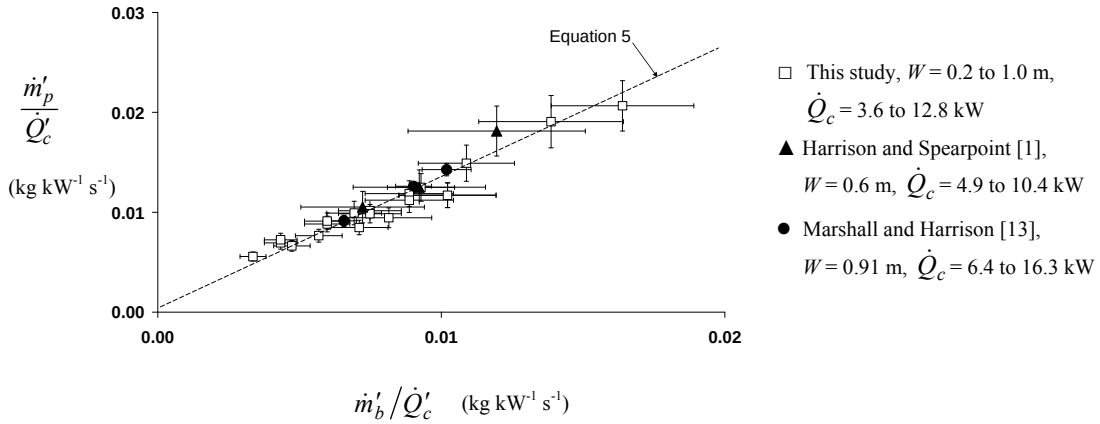

Fig. 4. Correlation between $\dot{m}'_p/\dot{Q}'_c$ and $\dot{m}'_b/\dot{Q}'_c$ at z = 0.

Figure 4 shows that all of the data, obtained from a range of $\dot{Q}_c$ and W, generally follow a relationship described by Equation 5, with regression coefficients of β = 1.34 and γ = 0. The standard error of the regression coefficient β is 0.023. This is similar to that suggested by Thomas et al [4] (i.e. β = 1.4) from analysis of much fewer data points. It seems reasonable to use Equation 5 to describe the entrainment of air into the flow below the balcony, instead of the regression coefficients β = 1.2 and γ = 0.0027 given in Equation 3, which were determined using multiple linear regression from data mainly obtained above the balcony. Equation 5 provides a simpler equation, from a more robust data set, which is not determined from data obtained above the balcony, nor is it weakly dependent on $\dot{Q}_c$.

$$\frac{\dot{m}'_p}{\dot{Q}'_c} = 1.34 \frac{\dot{m}'_b}{\dot{Q}'_c} \tag{5}$$

Therefore, Equation 6 is proposed to describe entrainment into 2-D balcony spill plumes, as it is a simpler, modified version of Equation 3 and does not require the calculation of both $\dot{m}_b$ and d_b as required by Equation 4 and appears to generally apply with respect to variation in $\dot{Q}_c$ and W.

$$\frac{\dot{m}'_{p,2D}}{\dot{Q}'_c} = 0.16\frac{z}{\dot{Q}'^{2/3}_c} + 1.34\frac{\dot{m}'_b}{\dot{Q}'_c} \qquad \text{or} \qquad \dot{m}_{p,2D} = 0.16\dot{Q}_c^{1/3}W^{2/3}z + 1.34\dot{m}_b \tag{6}$$

Balcony Spill Plume with Entrainment of Air into the Ends – The 3-D Plume

There is a limited amount of experimental data currently available for 3-D balcony spill plumes. Work by Harrison and Spearpoint [1] and Hansell et al [14], provides data from 1/10th scale model studies, which includes data describing the layer flow below the balcony edge. If the Harrison and Spearpoint data is correlated according to Equation 1, then;

$$\frac{\dot{m}'_{p,3D}}{\dot{Q}'_c} = 0.22\frac{z}{\dot{Q}'^{2/3}_c} + 1.92\frac{\dot{m}'_b}{\dot{Q}'_c} - 0.0042 \tag{7}$$

The Hansell et al data (which forms the basis of the guidance given in [2] and [3]) correlates to;

$$\frac{\dot{m}'_{p,3D}}{\dot{Q}'_c} = 0.34\frac{z}{\dot{Q}'^{2/3}_c} + 2.64\frac{\dot{m}'_b}{\dot{Q}'_c} - 0.0083 \tag{8}$$

The difference in α between Equations 7 and 8 (i.e. the 0.22 and the 0.34) provides significant differences in predicted entrainment. Possible reasons for this may relate to differences in the nature of the plume, fire compartment geometry or smoke reservoir geometry between each experimental study. Thus, there is currently uncertainty concerning an appropriate calculation method to predict the entrainment of air for the 3-D plume. To address this uncertainty, this work provides new data to systematically characterise entrainment of air into 3-D plumes. Figure 5 shows a plot of all the data from this study in a form consistent with the dimensional analysis by Thomas et al [4].

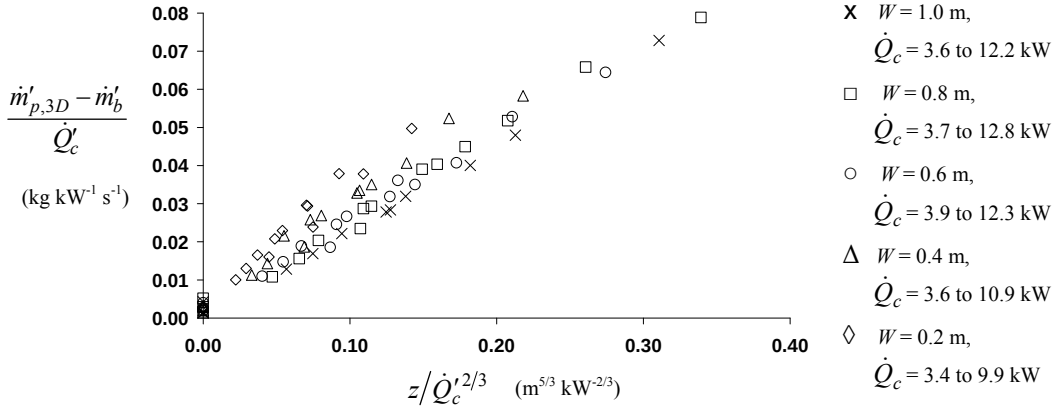

Fig.5. Comparison of mass flow rate with respect to height of rise according to Thomas et al [4]

Figure 5 shows some scatter of the data which appears to be dependent on *W*. The data exhibits linearity, with the representative slope of the line through each data set, for each value of *W*, appearing to increase as *W* decreases. The slope of the line represents the rate of entrainment with respect to height above the balcony. Figure 5 indicates that plumes generated from narrower openings tend to entrain air at a greater rate with respect to height, compared to plumes generated from wider openings. The difference in entrainment appears to be dependent on the nature of the rising plume. Figure 6 shows photographs of plumes generated in the scale model from both a wide and a narrow opening. Figure 6 shows that entrainment into the plume rising above the balcony can be considered in two distinct regions. The first region consists of entrainment into the 2-D region of the plume, rising above, and in line with the compartment opening. The second region is entrainment into both ends of the plume, which, based on visual observations, appeared to be more 3-D in nature, as the lateral extent of the plume increased with height above the balcony. It seems reasonable to expect that the rate of entrainment into the ends of the plume is greater than in the 2-D region of the plume. Figure 6 shows that the majority of the plume from

the wide opening consists of the 2-D region, with entrainment into the ends of the plume being less significant in the overall entrainment process. However, for the narrow opening, entrainment into the ends of the plume is more significant in the overall entrainment process. Therefore, it seems reasonable that narrow plumes entrain air at a greater rate with respect to height compared to wide plumes.

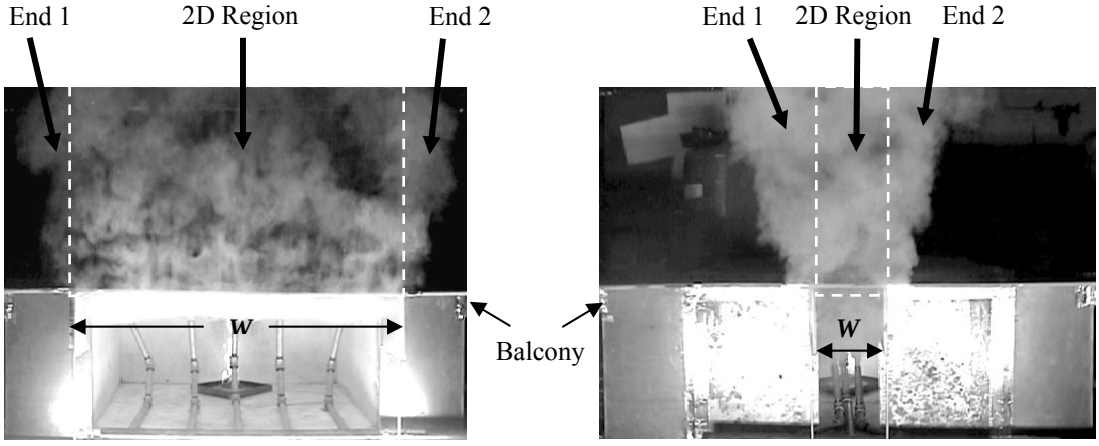

a) plume from a opening with $W = 1.0$ m b) plume from a opening with $W = 0.2$ m

Fig. 6. Photographs of the plume behaviour.

Figure 7 shows a plot of the experimental data according to Poreh et al [4] as given by Equation 2. Figure 7 shows that the general data set does not conveniently pass through the origin (as seen in Figure 3 for the 2-D plume) when an adjustment is made to the height of rise of the plume (assuming $z_o = d_b$).

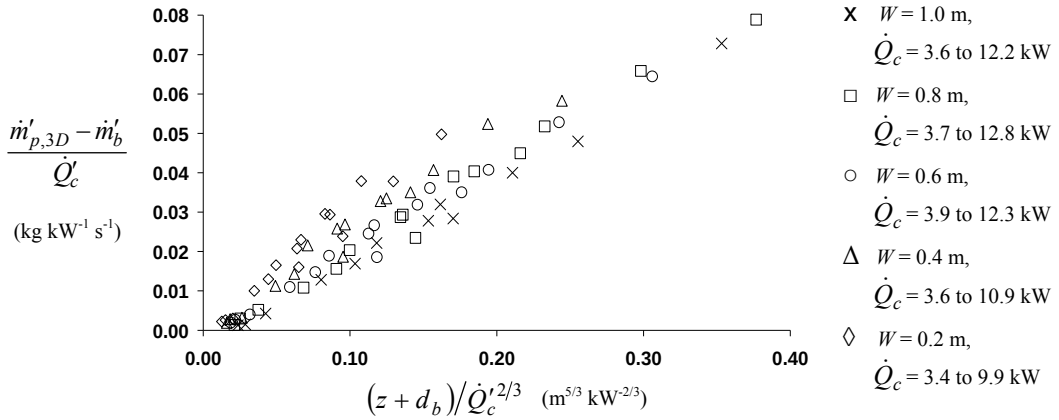

Fig. 7. Comparison of mass flow rates with respect to height of rise according to Poreh et al [5]

Figure 7 indicates that any line of best fit through each data set, for each value of W, would give rise to a negative intercept on the vertical axis. This negative intercept infers negative entrainment in the turning region, which is implausible. It appears that for the 3-D plume, the additional entrainment into the ends of the plume, gives rise to a different location of virtual origin (based on data obtained above the balcony) to that assumed in Equation 2. The location of this virtual origin is likely to be dependent on W as the contribution of the end entrainment changes. The use of Equation 2, which was developed for a 2-D plume, may not be appropriate for a 3-D plume, when encompassing the additional end entrainment into a 'lumped' entrainment coefficient for the entire plume above the balcony. Therefore, the Poreh et al method will not be considered further in this paper for the 3-D plume. The Thomas et al method [4], given by Equation 1, will be used in the analysis of the 3-D plume, as it does not make the fundamental assumption of a virtual origin. If the entrainment into the flow below the balcony is first considered, the values of the relevant regression coefficients β and γ, from previous work (as given in Equations 7 and 8), are dissimilar to those given by Equation 5 (i.e. $\beta = 1.34$ and $\gamma = 0$). However, as the values of β and γ given in Equations

7 and 8 were determined from data mainly obtained above the balcony, it is possible that, in the previous work, the additional entrainment into the ends of the plume (above the balcony) has been taken into account by modifying β and γ (as well as α) when linear regression is performed. It seems reasonable to assume that Equation 5 is appropriate to describe entrainment of air below the balcony for the 3-D plume, as, in the analysis, this entrainment was decoupled from the entrainment of air above the balcony. Because of this, the entrainment of air above the balcony has been treated separately in the analysis. To decouple the entrainment of air above the balcony, the measured mass flow rates were modified by subtracting the mass flow rate in the plume at $z = 0$ for each W and $\dot{Q}_t$ (and hence, $\dot{Q}_c$) examined. Thus, for each W, the data set passes through the origin, with the slope of each line representing the regression coefficient, α. Linear regression was performed to determine α with respect to W and $\dot{Q}_t$. Figure 8 shows the results of the linear regression with values of α (and associated standard errors) plotted with respect to W. The fixed value of α for the 2-D plume (i.e. 0.16 from Equation 6) is also shown.

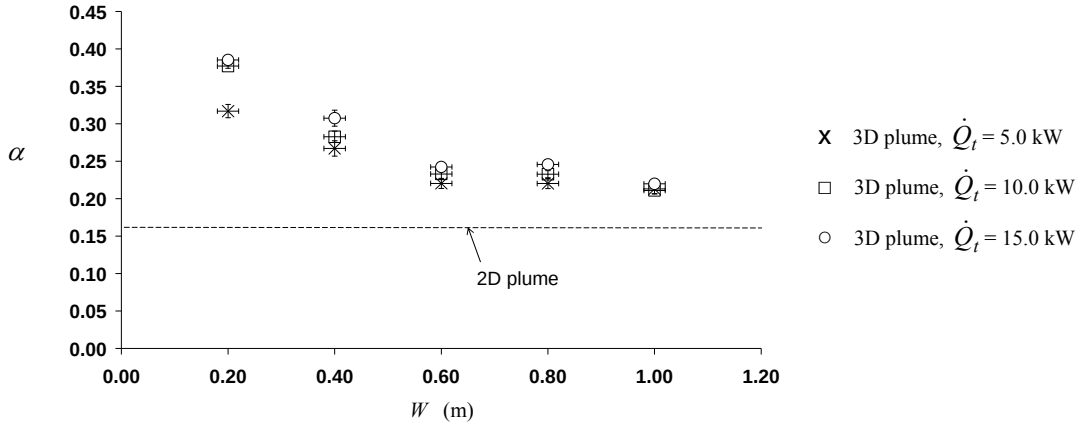

Fig. 8. Plot of α versus W, describing the rate of entrainment into the plume above the balcony edge

Figure 8 shows that when W = 1.0 m, α ≈ 0.21, which is slightly higher than α for the 2-D plume due to the additional end entrainment. As W decreases, α generally increases, with a maximum value of ≈ 0.38. The difference in α between the 3-D and 2-D plumes is representative of the amount of entrainment into the ends of the plume. Figure 8 shows that as W decreases, the contribution of end entrainment in the overall entrainment process increases, thus increasing the value of α, which is consistent with the analysis described above. For W = 1.0 m, Figure 8 shows that α appears to be independent of $\dot{Q}_t$. However, as W decreases, the value of α appears to become somewhat dependent on $\dot{Q}_t$. This is contrary to that observed for the 2-D plume. A possible reason for this may be due to the variation in d_b with respect changes in W and $\dot{Q}_t$. For wide openings, d_b was reasonably insensitive to changes in $\dot{Q}_t$, however, for narrow openings, the observed d_b was more sensitive to changes in $\dot{Q}_t$. It is possible that the amount of end entrainment is directly proportional d_b (also postulated by Thomas et al [4]). A deep layer rotating at the balcony edge will give rise to a plume which rises with broader ends compared to a shallow layer, thus entraining more air. Figure 9 shows a plot of (α_{3D}- α_{2D}) versus (W/d_b) to express the contribution of entrainment into the ends of the plume and to take into account the effect of d_b. Figure 9 shows that the data shown in Figure 8 now collapse to the relationship given by Equation 9.

$$(\alpha_{3D} - \alpha_{2D}) = 0.246\left(\frac{W}{d_b}\right)^{-0.687} \tag{9}$$

The standard errors of the regression coefficients 0.246 and -0.687 are 0.020 and 0.048 respectively. Therefore, for design purposes it seems reasonable and convenient to express Equation 9 by Equation 10.

$$(\alpha_{3D} - \alpha_{2D}) = 0.25\left(\frac{W}{d_b}\right)^{-2/3} \tag{10}$$

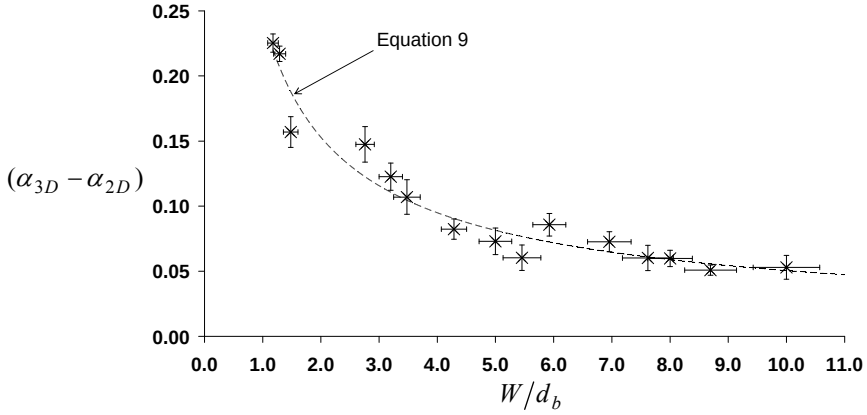

Fig. 9. Plot of (α_{3D}- α_{2D}) versus (W / d_b)

It appears that it is not appropriate to assign a universal value of α to represent the total amount of entrainment above the balcony due to the varying contribution of end entrainment. Therefore, to develop a general simplified design formula for the 3-D plume, an empirical formula was determined to explicitly describe the mass flow rate of gases into the ends of the plume above the balcony, which can be described by Equation 11.

$$\frac{\dot{m}'_{p,3D} - \dot{m}'_{p,2D}}{\dot{Q}'_c} = \frac{\dot{m}'_{ends}}{\dot{Q}'_c} = (\alpha_{3D} - \alpha_{2D})\frac{z}{\dot{Q}'^{2/3}_c} \quad \text{or} \quad \dot{m}_{ends} = (\alpha_{3D} - \alpha_{2D})\dot{Q}_c^{1/3} W^{2/3} z \tag{11}$$

If Equation 10 is substituted into Equation 11, this gives an explicit term to describe the mass flow rate of gases into the ends of the plume (Equation 12), which suggests that the amount of end entrainment is proportional to d_b.

$$\dot{m}_{ends} = 0.25\dot{Q}_c^{1/3} d_b^{2/3} z \tag{12}$$

Equation 12 was determined from data which exhibited linearity. It is expected that at higher heights of rise of plume, the effect of end entrainment will cause the plume to be more axisymmetric in nature and linearity will no longer apply. As Equation 12 is empirical in nature, the limit given by Equation 13 applies for its use.

$$\frac{z}{W} \leq 5 \tag{13}$$

A simplified design formula for the 3-D plume can now be deduced by simply appending Equation 12 to the design formula for the 2-D plume (given by Equation 6). Equation 14 describes the sum of entrainment of air into the flow below the balcony, entrainment into the 2-D region of plume above the balcony and entrainment into the ends of the plume above the balcony. Equation 14 applies to a flow which is channelled by screens beneath the balcony, with the limit given by Equation 13. The overall uncertainty in the use of Equation 14, will be dependent on the nature of the plume and hence, the relative contribution of each term and the associated standard error of each regression coefficient.

$$\begin{aligned} \dot{m}_{p,3D} &= 0.16\dot{Q}_c^{1/3} W^{2/3} z + 1.34\dot{m}_b + 0.25\dot{Q}_c^{1/3} d_b^{2/3} z \\ \Rightarrow \dot{m}_{p,3D} &= 0.16\dot{Q}_c^{1/3}(W^{2/3} + 1.56 d_b^{2/3}) z + 1.34\dot{m}_b \end{aligned} \tag{14}$$

This work suggests that entrainment of air into a 3-D balcony spill plume is dependent on the characteristics of the layer flow below the balcony edge and may explain differences between measured entrainment from previous studies. The Harrison and Spearpoint [1] data was determined from a flow with W = 0.6 m, whereas the Hansell et al [14] data was determined from flow which was narrower with $W \approx 0.43$ m. Thus, it appears that currently available simplified formulae for the 3-D plume, based on these data [given in references 1-3], apply specifically to the range of conditions studied in these experiments and do not apply generally for a wide range of W. Following the analysis of this work, it is not surprising that value of α obtained from Hansell et al [14] is greater than that obtained from Harrison and Spearpoint [1], as the plumes were generated from a narrower opening. This may explain the differences in entrainment between these previous studies and the use of Equation 14 may be appropriate to reconcile these differences. Therefore, Equation 14 was applied to the data from these previous studies, using the measured data for the layer flow below the balcony edge as the input. Figure 10 shows that Equation 14 provides a good prediction of the Harrison and Spearpoint experimental results. Equation 14 also provides a reasonably good prediction of the Hansell et al data for smaller values of mass flow rate, obtained at low heights of rise. However, for larger values obtained at higher height of rise, there is divergence between the experimental results and the prediction, with a general trend to under predict the experimental results. However, the experimental boundary conditions in the Hansell et al work were such that the nature of the plume was different to the unbounded plumes generated in this work and by Harrison and Spearpoint [1]. The plumes generated by Hansell et al were obtained from a model which had four asymmetric openings for inlet air, with the resulting plume having a tendency to become more axisymmetric in nature due to the observed swirling of rising plume in the smoke reservoir [5,14]. Therefore, due to the different nature of the plume, it is possible that the Hansell et al can be considered to be anomalously high (particularly for larger heights of rise of plume) compared to the data obtained from the unbounded spill plumes in this work and by Harrison and Spearpoint [1]. Therefore, it appears that Equation 14 goes some way to reconcile the differences in entrainment between previous work and can be applied more generally compared to currently available simplified design formulae.

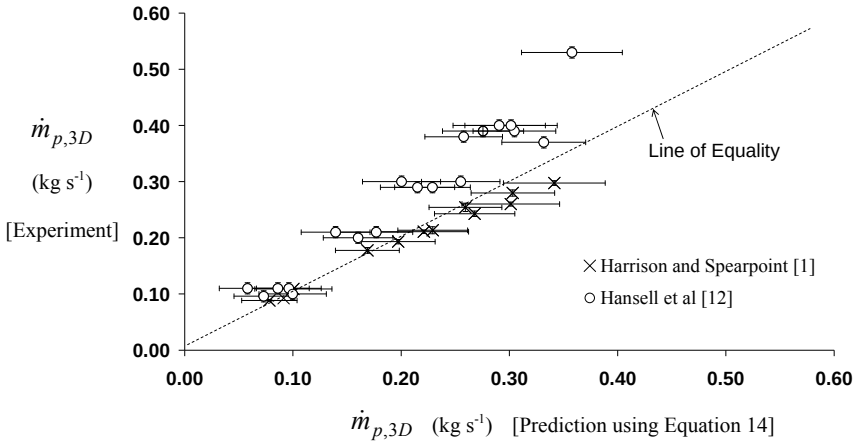

Fig. 10. Comparison of experiment and prediction of $\dot{m}_{p,3D}$ (using Equation 14) from previous studies

CONCLUSIONS

This work has provided new experimental data to systematically characterise entrainment of air into a balcony spill plume generated from a flow which is channelled by screens beneath the balcony. This work has demonstrated that existing simplified design formulae, for the 2-D balcony spill plume, apply generally for plumes generated from a range of fire compartment geometries. A further simplified design formula is presented for the 2-D plume. The rate of entrainment into a 3-D balcony spill plume appears to be specifically dependent on the characteristics of the layer flow below the balcony edge. 3-D plumes generated from narrow openings entrain air at a greater rate with respect to height compared to those generated from wider openings. The rate of entrainment appears to be dependent on the contribution of the end entrainment in the overall entrainment process. A simplified design formula is proposed for the 3-D plume, by developing a general empirical expression to explicitly describe the entrainment of air into the

ends of the plume. This simplified formula can be applied more generally compared to currently available formulae for the 3-D plume. This work goes some way to explain and reconcile differences in entrainment reported between previous studies and provides improved guidance to designers of smoke management systems.

ACKNOWLEDGEMENTS

The authors would like to thank the following: Education New Zealand, for awarding the lead author a New Zealand International Doctoral Research Scholarship. The National Fire Protection Association for awarding the lead author the David B. Gratz Scholarship. Bob Wilsea-Smith and Grant Dunlop of the University of Canterbury, for their help with the design and construction of the experimental apparatus. The New Zealand Fire Service Commission for their continued support of the Fire Engineering programme at the University of Canterbury.

REFERENCES

[1] Harrison, R. and Spearpoint, M.J., "Entrainment of Air into a Balcony Spill Plume", Journal of Fire Protection Engineering, Vol. 16, No. 3, 2006, pp 211-245. doi:10.1177/1042391506057954

[2] NFPA 92B, "Smoke Management Systems in Malls, Atria and Large Areas," 2005 Edition, Publication No 92B, National Fire Protection Association, Quincy, MA, USA, 2005.

[3] Chartered Institution of Building Services Engineers, *CIBSE Guide Volume E: Fire Engineering*, London, CIBSE, 2003.

[4] Thomas, P.H., Morgan H.P. and Marshall N.R., "The Spill Plume in Smoke Control Design," Fire Safety Journal, Vol. 30, No. 1, 1998, pp 21-46. doi:10.1016/S0379-7112(97)00037-4

[5] Poreh, M., Morgan, H.P., Marshall N.R. and Harrison R., "Entranment by Two Dimensional Spill Plumes in Malls and Atria," Fire Safety Journal, Vol. 30, No. 1, 1998, pp 1-19. doi:10.1016/S0379-7112(97)00036-2

[6] Morgan, H.P., Ghosh, B.K., Garrad, G., Pamlitschka, R., De Smedt, J-C. and Schoonbaert, L.R., "Design Methodologies for Smoke and Heat Exhaust Ventilation," BRE Report 368, Building Research Establishment, Watford, UK, 1999.

[7] Kumar S., Thomas, P.H., and Cox G., "Revised BRE Method for Spill Plume Entrainment Analysis," *Proceedings of the Second International Conference Fire Bridge*, University of Ulster, May 2005.

[8] Thomas, P.H., Hinkley, P.L., Theobald, C.R. and Simms, D.L., "Investigations into the Flow of Hot Gases in Roof Venting," Fire Research Technical Paper No 7, London, The Stationary Office, 1963.

[9] Marshall, N.R., "The Behaviour of Hot Gases Flowing within a Staircase," Fire Safety Journal, Vol. 9, No 3, 1985, pp 245-255. doi:10.1016/0379-7112(85)90035-9

[10] Klote, J.H., and Milke, J.A., *Principles of Smoke Management,* Chapter 15, Physical Modeling, ASHRAE, Atlanta, GA, 2002.

[11] Zukoski, E.E., Kubota, T. and Cetegen, B., "Entrainment in Fire Plumes," Fire Safety Journal, Vol. 3, No.3, 1981, pp 107-121. doi:10.1016/0379-7112(81)90037-0

[12] Lee, S.L., and Emmons, H.W., "A Study of Natural Convection above a Line Fire," Journal of Fluid Mechanics, Vol. 11, No 3, pp 353-368, 1961. doi:10.1017/S0022112061000573

[13] Marshall, N.R. and Harrison, R., "Experimental Studies of Thermal Spill Plumes", Building Research Establishment Occasional Paper, OP1, 1996.

[14] Hansell, G.O., Morgan, H.P. and Marshall, N.R., "Smoke Flow Experiments in a Model Atrium," BRE Occasional Paper OP55, Building Research Establishment, Watford, UK, 1993.